JOURNAL OF MATERIALS SCIENCE 21 (1986) 2965–2971

The orientation of molecules at the locus of failure of polymer coatings on steel

J. F. WATTS, J. E. CASTLE, S. J. LUDLAM
Department of Materials Science and Engineering, University of Surrey, Guildford, Surrey GU2 5XH, UK

The technique of angular resolved electron spectroscopy has been applied to the analysis of the failure surfaces generated by the cathodic disbondment of epoxy coatings on mild steel. It is shown that failure occurs adjacent to the epoxy group of the bisphenol A epoxy chain. These groups present at the locus of failure then segregate with the metal side of the failed couple. Complementary results are seen on the polymer side of the failure, the outer nanometre apparently being depleted in epoxy groups.

1. Introduction

X-ray photoelectron spectroscopy (XPS) is now a well established technique for the quantitative evaluation of the surface and near surface composition of materials. The use of XPS in polymer-to-metal adhesion studies and elucidation of the associated failure modes has been explored in a series of communications from this laboratory [1–4]. In this paper the use of angular resolved photoelectron spectroscopy to determine near surface concentration gradients is described.

A recent investigation [4] of the failure mode of two epoxy copolymers applied to the mild steel panels, following mechanical testing and cathodic disbondment in saline solution, has shown that failure occurs close to, but not at, the polymer–metal interface. The quantitative surface analyses were very similar irrespective of the mode of inducing failure. By curve fitting of the high resolution C1s spectra it became clear that there were subtle differences between surfaces obtained by mechanical delamination and saline exposure. Those panels which had been treated in aqueous solution showed displacement of epoxy species from the metal surface and a complementary enhancement of epoxy residues was observed on the interfacial polymer surface. Following mechanical failure, spectra from the metal and polymer surfaces showed no such segregation of organic residues. The behaviour in aqueous solution is consistent with that predicted by surface thermodynamics for an epoxy polymer on an oxidized iron substrate [5], i.e. that disbondment of hydrophilic surfaces will occur. The polymeric overlayer remaining on the metal substrate was thin (2 to 4 nm) and contained epoxy groups. It was unclear however where these were located with respect to the free surface.

Clearly a knowledge of the concentration gradients that exist within these thin overlayers would be invaluable in defining the locus of failure more accurately. The usual way of obtaining a compositional depth profile in electron spectroscopy is by *in situ* erosion of the sample surface by a beam of inert gas ions, carried out sequentially with the analysis technique until the required depth is reached [6]. This method is unsuitable for polymers owing to problems of sample degradation and consequently a non-destructive method of depth profiling must be sought. This can be achieved in XPS by varying the electron emission angle (take-off angle), the maximum depth of analysis being achieved normal to the sample surface and the minimum depth at grazing incidence [7–9]. There is a minimum useful value of grazing incidence ($\theta = 15°$) below which instrumental constraints may distort the angular profile.

In this paper we report the use of angular XPS to resolve the uncertainties concerning the exact position of the remaining epoxy groups and hence define the locus of failure more accurately.

2. Experimental procedure

2.1. Specimen preparation and analysis

These details have been given elsewhere [4] and will only be outlined in this section. Epoxy-acrylic or epoxy-phenolic coatings were applied to diamond polished mild steel panels approximately 1 mm thick. The work described in [4] used much thinner test panels which led to interfacial segregation of manganese; this is avoided by the use of these thicker panels. The panels were polished to a mirror finish prior to coating to improve angular resolution. The coated panels were cut into strips 1 cm wide, immersed in 0.5 M NaCl solution, and cathodically polarized at -1300 to -1500mV (against standard calomel electrode, SCE) for several hours. After treatment the coating was stripped off using adhesive tape and mirror images of the failure interface were analysed by XPS. Photoelectron spectroscopy was carried out using a VG Scientific ESCA3 MkII, employing Al$K\alpha$ radiation. The one departure from previous practice was to reduce the analyser slit width to 2 mm, giving an analyser acceptance angle of approximately 6.5°. Spectra were recorded at electron take-off angles of 15°, 25°, 35°, 45° and 60° relative to the sample surface. The C1s spectra were resolved into three component peaks (C–H, C–O, and C=O) using an

0022–2461/86 $03.00 + .12

iterative least squares fitting routine. A quantitative surface analysis could then be calculated for each specimen, for each of the five take-off angles. The computer routine described in the next section was then used to calculate a matching angular profile from a postulated depth profile.

2.2. Computer modelling of the XPS angular profile

Before describing the methodology of modelling the XPS angular profile in detail, it is pertinent to review the basis of angular XPS and its application to defining near surface concentration gradients. If we consider an infinitely thick homogeneous material, the flux of electrons, I_d, derived from a depth d below the surface, is related to the total yield of electrons from that material, I_∞, by the well known Beer–Lambert expression:

$$I_d = I_\infty \exp\left(\frac{-d}{\lambda \sin\theta}\right) \quad (1)$$

where λ is the inelastic mean free path (attenuation length) for the electron energy and material, and θ is the electron take-off angle relative to the sample surface. (The electron take-off angle may be defined relative to the sample surface, when $\sin\theta$ appears in Equation 1, or the surface normal, when a $\cos\theta$ term is included. In this work we follow the convention of [7–9] and adopt the former definition.) It is a simple matter to manipulate this equation to calculate the thickness of thin uniform overlayers as demonstrated by Castle [10] for oxide layers on metals. This approach was adopted in our previous work to calculate the thickness of the polymer overlayers remaining on the steel substrate. When dealing with polymeric systems, however, the concentration gradients present are not seen as conveniently uniform overlayers, but as discrete changes in the atomic and molecular species present (C–H, C–O, C=O, O etc.). The solution to this dilemma is to consider the analysis volume as a series of steps or slices (i.e. very thin discrete overlayers). The electron emission for each slice can be calculated, as can the electron attenuation as a result of the slices above it. This can be repeated in turn for each element or molecular species present in the analysis. Thus by postulating a depth profile it is possible to set up the various equations and undertake the calculations to predict the angular profile it will generate.

The computer routine we have employed to undertake this task is closely based on the formalism of Paynter [9], which can be stated in a generalized form for a model profile with j steps, considering a single element, as follows:

$$I_\theta = kF\lambda \sin\theta \left\{ n_1 + \sum_{N=1}^{j} \lambda \sin\theta \left(\frac{n_{N+1} - n_N}{x_{2N} - x_{2N-1}}\right) \times \left[\exp\left(\frac{-x_{2N-1}}{\lambda \sin\theta}\right) - \exp\left(\frac{-x_{2N}}{\lambda \sin\theta}\right)\right]\right\} \quad (2)$$

where kF is an instrumental constant and is eliminated in the calculations, n_N is the atomic concentration at depth x_N, λ is the electron inelastic mean free path.

To define a system fully, the algorithm is expanded for the j steps for the appropriate number of take-off angles (in this case five) and molecular species (in this analysis seven; C–H, C–O, C=O, O, Fe, Na, Cl). Because of the large number of independent variables in the algorithm it is not possible to start with an angular XPS profile and work backwards to a unique compositional depth profile. The angular profile must be calculated from the postulated depth profile and compared with the experimental data. This procedure is then repeated on a trial and error basis until there is good agreement between calculated and experimental data.

In summary, the production of a composition depth profile in the manner described above involves many experimental and computational stages. These are described in the flow diagram of Fig. 1.

3. Results

Although the primary aim of this investigation was to establish the orientation of the residual polymer layers on the steel substrates, the contributions of iron, sodium and chlorine to the angular profile have also been included for completeness. This also provides us with a means of assessing the potential problems involved in applying such a technique to complex spectroscopic data from a materials science investigation.

3.1. Epoxy-acrylic resin applied to cathodically polarized mild steel

If we first consider the change in structure of the C1s spectrum with electron take-off angle, this becomes apparent following curve fitting of the spectra. The carbon spectra from the interfacial metal surface are shown in Fig. 2 for θ = 15°, 35°, 60°. The change in the relative intensities of the epoxy () component at approximately 286.6 eV and the carbonyl (C=O) component at 288.6 eV is clearly seen, the epoxy signal being somewhat greater at the more surface sensitive value of θ (15°). Following the convention of our previous investigation [4], we define a C–O/C=O value to enable comparison between spectra; this value is given in the caption.

The next stage in the analysis is to calculate a quantitative surface analysis using the photoelectron peak areas and the appropriate sensitivity factors. In the case of carbon the curve-fitting data are used to make a quantitative evaluation of the different organic groups present. The angular profile produced for the metal surface is presented in tabular form in Table I.

TABLE I Experimental angular profile for the interfacial metal surface of epoxy-acrylic coated mild steel following failure

θ	Atomic %						
	C–O	C=O	C–H	O	Fe	Na	Cl
15	4.75	2.67	56.67	23.80	5.20	3.80	3.11
25	4.35	3.19	59.75	23.80	4.30	2.60	2.01
35	3.36	2.55	47.80	33.80	6.50	3.30	2.69
45	2.27	2.09	38.70	46.40	6.00	2.60	1.94
60	2.65	2.47	48.17	32.30	6.50	2.60	5.31

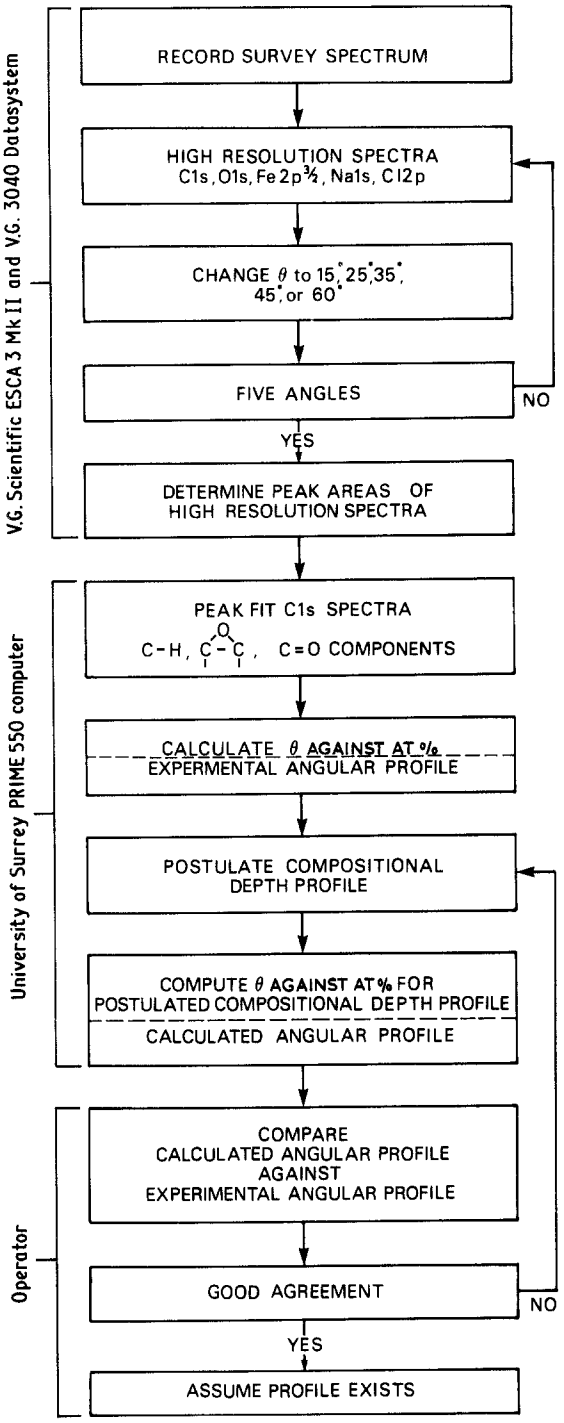

Figure 1 Flow diagram showing the stages necessary to produce a composition depth profile by the angular XPS method employed in this paper.

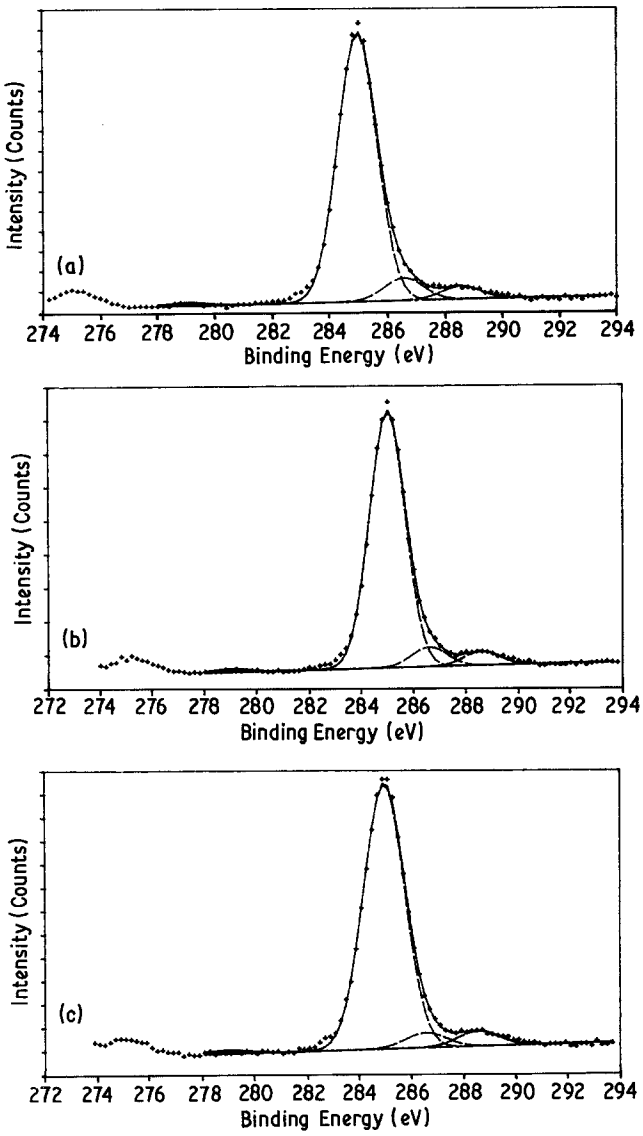

Figure 2 C1s spectra of the interfacial metal surface of the epoxy-acrylic coating. (a) C–O/C=O = 1.76, recorded at θ = 15°; (b) C–O/C=O = 1.38, recorded at θ = 35°; (c) C–O/C=O = 1.06, recorded at θ = 60°.

Using the computer routine described in Section 2.2. a composition depth profile is deduced from which a calculated angular profile showing close agreement with Table I is obtained (Table II). As the match of the experimental and calculated data for the organic substituent groups is particularly important, the values of C–O/C=O are compared graphically in Fig. 3. It can be seen that the agreement is good, both sets of data following the same trend.

This procedure was repeated for the polymer side of the failure and the three sets of data, experimental angular profile, depth profile, and calculated angular profile are presented in Table III.

The most significant difference between the data sets of Tables II and III is the change in the concentration of epoxy groups with depth. There is an enhancement of epoxy groups in the outer 1 nm of the overlayer present on the metal surface and a complementary depletion in the outer 1 nm of the interfacial polymer surface. Clearly it is easier to appreciate

TABLE II Postulated depth profile and the angular profile calculated from it

Parameter	Atomic %						
	C–O	C=O	C–H	O	Fe	Na	Cl
Calculated angular profile θ							
15	4.68	3.02	56.16	24.34	5.43	3.81	2.56
25	3.78	2.79	53.33	27.66	5.84	3.55	3.05
35	3.26	2.57	50.87	30.35	6.28	3.31	3.35
45	2.94	2.40	48.96	32.35	6.66	3.13	3.55
60	2.66	2.24	47.03	34.32	7.08	2.93	3.74
Depth (nm)							
0.0	8.00	1.00	60.00	20.00	5.00	4.00	2.00
0.7	4.50	5.00	57.00	23.00	5.20	4.00	1.30
1.5	2.75	3.00	55.00	26.00	6.00	3.00	4.25
2.5	1.00	2.00	50.00	33.80	6.50	2.00	4.70
3.5	1.00	1.00	42.00	45.00	6.00	1.50	3.50
5.0	1.00	1.00	30.00	50.00	12.00	1.00	5.00

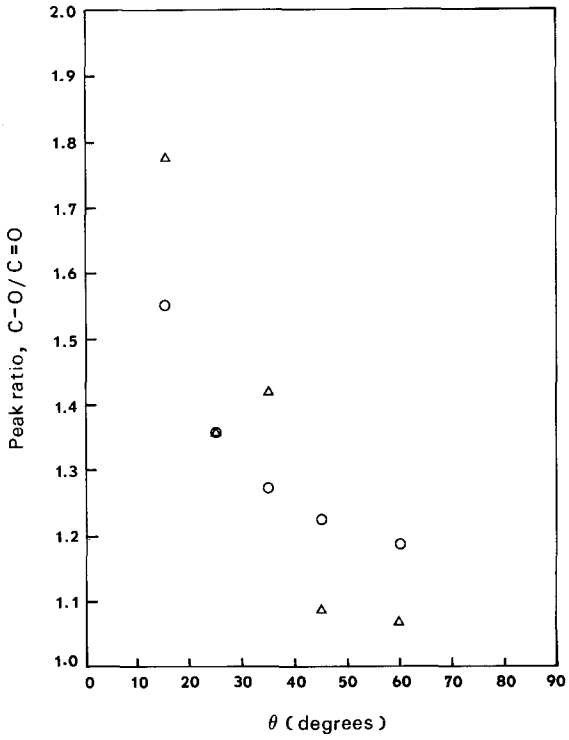

Figure 3 Values of C−O/C=O for the interfacial metal surface of the epoxy-acrylic coating from experimental data (△) and calculated by the computer routine (○).

a depth profile when it is presented in graphical form, and Fig. 4 shows the data of Tables II and III in this manner. The disadvantage of this form of presentation is that small (< 5%) changes in concentration are not immediately apparent, and for this reason the depth profiles are reproduced in both tabular and graphical form. The cumulative profile of Fig. 4 allows large changes to be easily seen, the area of each section of the graph representing the concentration of an atomic species as a function of depth.

3.2. Epoxy-phenolic resin applied to cathodically polarized mild steel

The experimental angular profiles, together with depth profiles and calculated angular profiles, for the interfacial metal and polymer surfaces are given in Tables IV and V, respectively. Once again it is informative to compare the experimental values of C−O/C=O graphically with those calculated from the depth profile. This is shown in Fig. 5 for both the metal and polymer surfaces. The enhancement of epoxy groups at the very near surface of the metal side and depletion on the polymer side is clearly seen as a change from positive to negative slope.

Cumulative compositional profiles to a depth of 5 nm either side of the locus of failure (Fig. 6) show the same trends as those for the epoxy-acrylic. The reduction of epoxy groups with depth is somewhat smaller on the metal surface (≃ 3 at %) and is not readily apparent from this graph, but is clearly seen in Table IV.

TABLE III Epoxy-acrylic coating interfacial polymer surface.

Parameter	Atomic %						
	C−O	C=O	C−H	O	Fe	Na	Cl
Experimental angular profile θ							
15	8.16	1.75	64.38	21.10	0.70	2.80	1.11
25	9.01	1.95	64.43	19.40	0.90	3.40	0.91
35	9.86	1.66	64.17	19.40	0.80	2.80	1.31
45	9.63	1.79	65.58	18.10	0.90	2.80	1.20
60	8.77	1.93	67.09	17.70	0.60	2.50	1.41
Calculated angular profile θ							
15	8.18	1.82	64.33	21.04	0.80	2.66	1.17
25	8.97	1.82	64.89	19.85	0.77	2.56	1.13
35	9.37	1.82	65.60	18.96	0.76	2.40	1.09
45	9.59	1.83	66.22	18.30	0.75	2.25	1.06
60	9.75	1.84	66.90	17.65	0.74	2.09	1.03
Depth profile (nm)							
0.0	4.50	1.90	65.00	25.00	0.90	2.00	0.70
0.7	9.00	1.75	64.00	20.00	0.85	2.80	1.60
1.5	10.00	1.95	64.00	19.00	0.70	3.40	0.95
2.5	10.00	1.66	64.00	19.00	0.70	2.80	1.84
3.5	14.00	1.79	65.58	15.00	0.70	2.80	0.13
5.0	10.00	1.93	74.00	12.00	0.70	0.50	0.87

4. Discussion

Both sets of data, for the epoxy-acrylic and epoxy-phenolic resins, show that there is an enhancement of

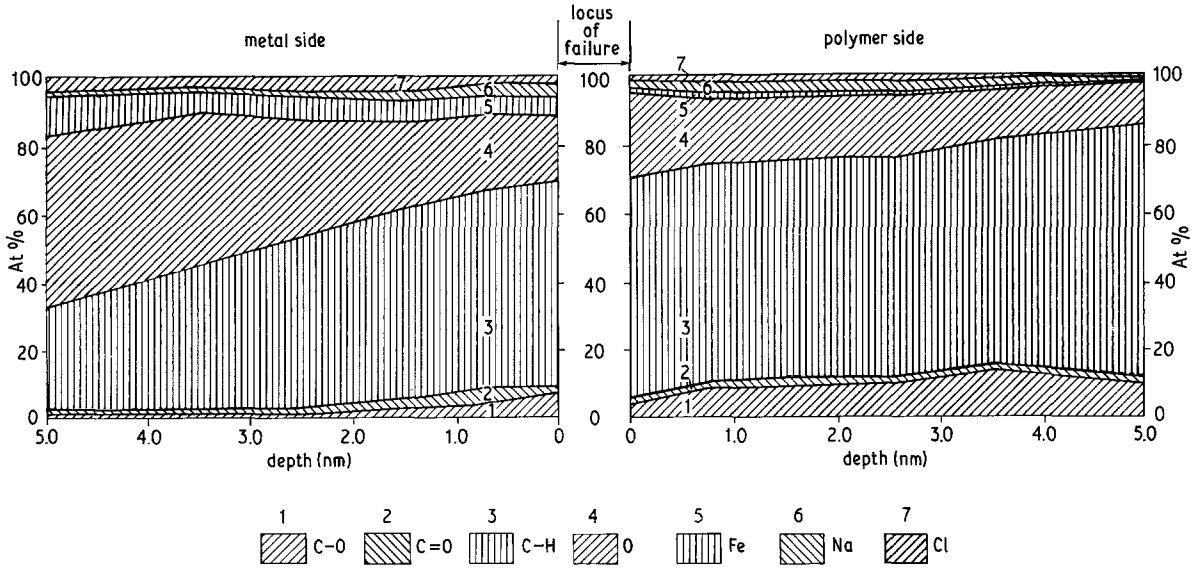

Figure 4 Compositional depth profile away from the locus of failure for the epoxy-acrylic resin.

TABLE IV Epoxy-phenolic coating interfacial metal surface.

Parameter	Atomic %						
	C–O	C=O	C–H	O	Fe	Na	Cl
Experimental angular profile θ							
15	4.46	2.44	56.38	25.60	4.80	3.60	2.72
25	4.51	2.70	50.38	29.50	5.00	4.50	3.41
35	4.20	2.60	52.61	29.00	5.70	3.20	2.69
45	3.90	2.45	51.38	30.00	7.20	4.50	0.57
60	3.67	2.53	53.68	28.90	7.10	2.50	1.62
Calculated angular profile θ							
15	4.43	2.73	56.22	25.74	4.71	3.55	2.61
25.	4.15	2.65	54.76	27.21	5.94	3.01	2.29
35	3.96	2.59	54.02	28.14	6.60	2.67	2.01
45	3.82	2.56	53.60	28.76	7.00	2.45	1.82
60	3.70	2.52	53.25	29.33	7.33	2.25	1.64
Depth (nm)							
0.0	5.10	3.00	63.00	22.50	1.50	4.00	0.90
0.7	4.50	2.70	56.00	25.00	2.50	5.00	4.30
1.5	4.10	2.60	50.00	29.00	9.00	2.00	3.00
2.5	3.50	2.45	51.00	31.00	9.00	2.00	1.05
3.5	3.00	2.30	51.00	33.00	9.50	1.00	0.20
5.5	2.80	2.30	51.50	33.00	9.00	1.00	0.40

TABLE V Epoxy-phenolic coating, interfacial polymer surface.

Parameter	Atomic %						
	C–O	C=O	C–H	O	Fe	Na	Cl
Experimental angular profile θ							
15	5.20	2.90	67.50	21.50	0.40	1.70	0.80
25	6.50	2.70	66.70	21.10	0.80	1.70	0.50
35	10.80	1.73	60.70	22.90	0.70	1.90	1.27
45	10.80	1.27	59.90	22.10	0.90	2.00	3.03
60	10.70	1.31	60.70	22.40	0.90	2.70	1.29
Calculated angular profile							
15	5.19	2.90	66.64	21.55	0.58	1.61	1.54
25	7.43	2.18	64.14	21.81	0.66	2.00	1.78
35	8.83	1.79	62.47	22.02	0.70	2.28	1.92
45	9.74	1.54	61.34	22.18	0.73	2.48	1.99
60	10.56	1.33	60.30	22.35	0.76	2.66	2.04
Depth (nm)							
0.0	1.00	6.00	70.00	20.50	0.40	1.10	1.00
0.7	2.00	2.50	70.00	22.00	0.50	1.20	1.80
1.5	11.00	1.00	63.00	22.00	0.70	1.90	0.40
2.5	14.00	0.50	57.00	22.00	0.90	2.50	3.10
3.5	14.00	0.10	55.00	22.40	0.90	3.50	4.10
5.5	16.00	0.10	53.00	24.00	0.90	4.00	2.00

epoxy groups in the outer surface layers (1 nm) of the polymer overlayer on the metal surface and a complementary depletion on the polymer side of the failure. At first sight this would seem to be in direct contradiction to the results of our previous investigation [4], where depletion at the metal surface and enhancement on the polymer were reported, however this is not the case. Our previous work was carried out at constant take-off angle (45°) and as a result the analysis was averaged over a depth of about 3 to 4 nm. The assumption implicit in our treatment of the data was that the specimen was homogeneous within the depth probed by XPS. This is clearly not the case, but it is an assumption regularly made in quantitative XPS to allow direct comparison between data from similar specimens. The phenomenon previously observed (i.e. enhancement of epoxy groups on the polymer surface and depletion on the metal surface) is still clearly apparent from the data of Tables I, III, IV and V recorded at the higher take-off angles (45° and 60°). The analytical data presented in this paper presents a more complete view of the locus of failure in that it reveals the orientation of the epoxy groups in that region.

Both coatings are based on bisphenol A epoxy resins with various copolymer substituents [4], links

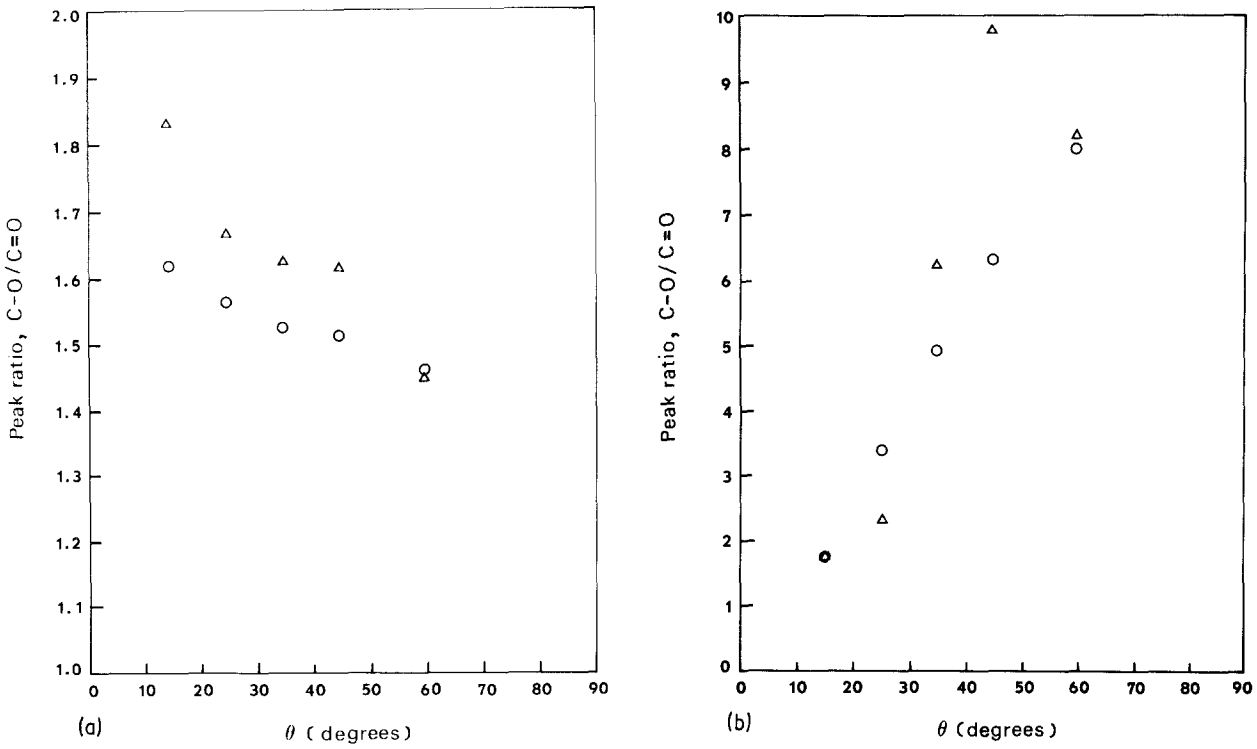

Figure 5 Experimental (△) and calculated (○) values of C–O/C=O for the (a) epoxy-phenolic interfacial metal, and (b) polymer surfaces.

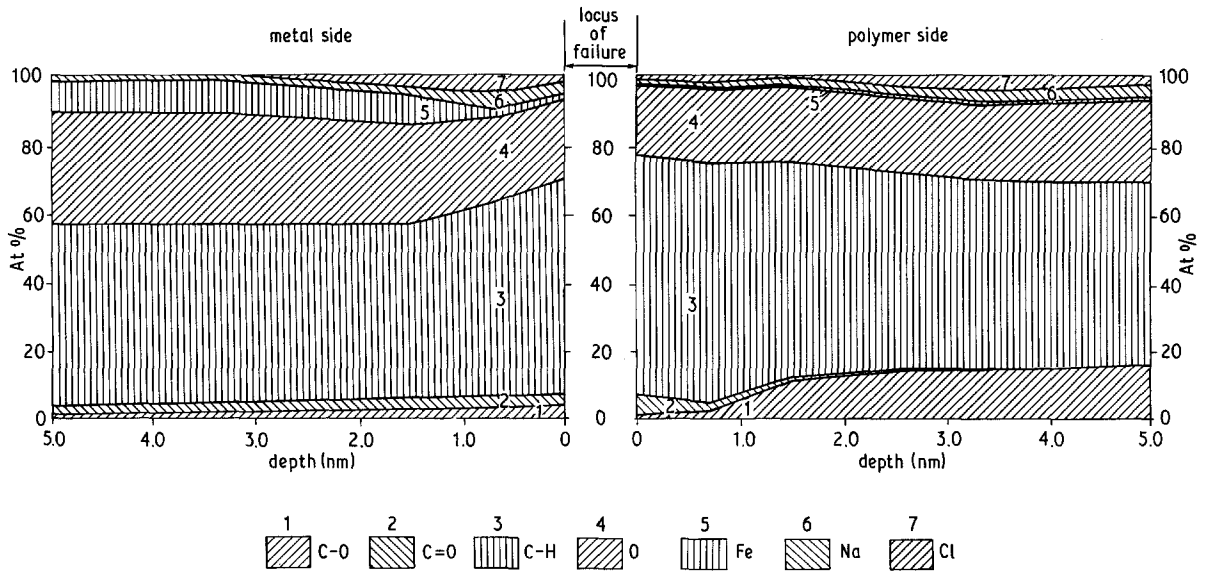

Figure 6 Compositional depth profile away from the locus of failure for the epoxy-phenolic resin.

between them are provided by various pendant groups along the bisphenol A epoxy repeat unit:

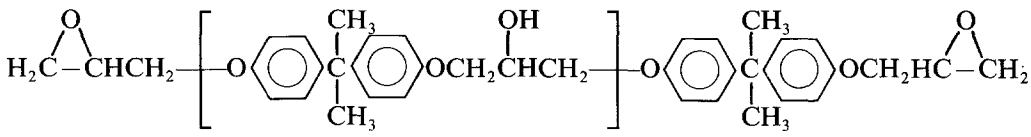

The experimental data indicates that the locus of failure follows a well defined route, chain scission occurring adjacent to the epoxy groups which remain at the interfacial surface of the thin polymer overlayer remaining on the metal substrate.

There are two possible scenarios that would bring about results of this type; the first is a major reorientation of the molecules at the polymer–metal interface. Failure can then occur at equivalent points on the polymer chain leaving a uniform overlayer of polymer on the metal surface terminating in epoxy groups (Fig. 7a). Alternatively the random orientation of the molecules may bring about a non-uniform overlayer as illustrated in the simplified schematic of Fig. 7b. In this case failure still occurs at epoxy groups on the polymer chain, a feature common to both models. It is probable that pendant groups along the molecules which provide the links with other chains define the locus of failure resulting from the action of the cathodically generated alkali (NaOH). If we consider the epoxy-acrylic resin in the presence of the alkali, failure will occur as follows:

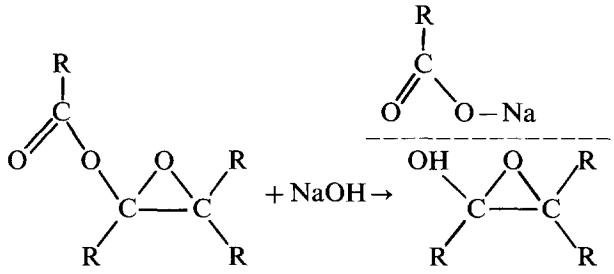

the dotted line indicating the locus of failure.

Of the two failure schemes of Fig. 7 the latter is more likely. The only opportunity for the polymer chains to reorientate themselves is during stoving at elevated temperature; however the mechanism of curing relies on the crosslinking of the bisphenol A epoxy chains with the other copolymer constituents thus reducing their mobility, consequently the gross reorientation described by Fig. 7a is extremely

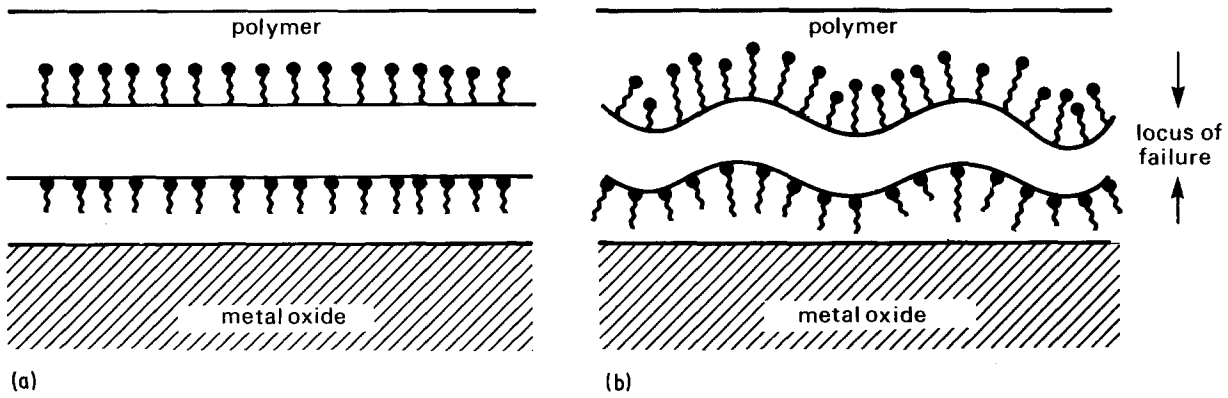

Figure 7 Schematic representation of possible failure modes showing (a) the effect of re-orientation and (b) random orientation, of the molecules close to the polymer–metal oxide interface. ●, epoxy group; ~, hydrocarbon chain.

unlikely, However, it is conceivable that a weak boundary layer is formed during stoving by the segregation of molecules low in epoxide to the interface zone. Failure occurs a similar distance from the metal oxide–polymer interface during both dry and aqueous tests [4]. In the case of failure following aqueous exposure, a hydrophilic route is taken. Molecules on the metal side are pinned, by their interaction with the metal substrate, sufficiently to prevent *in vacuo* reorientation. On the polymer side of the failure molecular reorientation [11] leads to the surface adopting a hydrophobic configuration, observed in our analyses as a depletion of surface epoxy groups. This is particularly clear from the epoxy profile on the polymer side of the failure of the epoxy-phenolic resin (Fig. 6). It is now informative to consider the depth profiles (Figs 4 and 6) for information at an elemental level which supports the hypothesis of Fig. 7b.

The iron signal of Table I shows little variation with take-off angle, and our routine (which necessarily assumes lateral homogeneity) reconstructs a depth profile (Fig. 4) with a small amount of iron present which remains constant until a depth of about 4 nm. An alternative interpretation is that of a non-uniform overlayer; in places the polymer overlayer is very thin, but elsewhere it is thicker, (Fig. 7b) thus lending further support to this model of failure.

The concentration of sodium on the metal side of the failure decreases with depth, which is to be expected from our previous work. Water is cathodically reduced to hydroxyl ions at the metal surface [2], the sodium acting as a counter-ion, and the concentration distribution represents the diffusion of Na^+ towards the interface. This trend is continued on the polymer side, although here the sodium is also attached to the polymer surface following failure as described in our proposed failure mechanism. The chlorine concentration present in the epoxy-acrylic resin is much lower than the sodium, (representing excess sodium chloride, the sodium assay being the sum of the chloride and hydroxide), but the depth distribution curve is of a similar type. The oxygen portion of the compositional depth profile is obviously a convolution of both inorganic oxygen (as the substrate iron oxide) and the organic oxygen of the polymeric coatings. Some oxygen will be present as the hydroxide following the electrochemical reduction of water and oxygen.

5. Conclusions

When the failure of epoxy-acrylic and epoxy-phenolic resins is brought about by cathodic polarization, delamination occurs adjacent to the epoxy groups in the polymer chain and possibly within a weak boundary layer. These epoxy groups remain outermost on the very thin polymeric overlayer remaining on the steel substrate but on the polymer side may become reoriented in the vacuum of the spectrometer. There is no evidence for gross orientation of the molecules in the interphase region during stoving. The thickness of the overlayer following failure varies in a random manner as described by Fig. 7b.

This work has also presented an opportunity to assess the utility of angular resolved electron spectroscopy in a materials science context. Although these results do not present the unambiguous surface crystallographic information available from simple systems, they do yield unique information concerning the orientation of molecules at the locus of failure. We are convinced that modelling angular XPS depth profiles in this manner provides a valuable extension of the XPS technique in materials science.

Acknowledgements

The authors wish to thank Dr R. W. Paynter, Université Laval, Quebec, Canada for the provisions of the computer program and Dr F. R. Jones for invaluable discussions.

References

1. J. F. WATTS and J. E. CASTLE, *J. Mater. Sci.* **18** (1983) 2987.
2. *Idem, ibid.* **19** (1984) 2259.
3. J. F. WATTS, *ibid.* **19** (1984) 3459.
4. J. E. CASTLE and J. F. WATTS, *Ind. Eng. Chem. Prod. Res. Dev.* **24** (1985) 361.
5. A. J. KINLOCH and R. A. GLEDHILL, *J. Adhesion* **6** (1974) 315.
6. S. HOFFMAN, in "Practical Surface Analysis by Auger and X-ray Photoelectron Spectroscopy" edited by D. Briggs and M. P. Seah (Wiley, Chichester, 1983) p. 141.
7. C. S. FADLEY, *J. Elec. Spec.* **5** (1974) 725.
8. M. PIJOLAT and G. HOLLINGER, *Surf. Sci.* **105** (1981) 114.
9. R. W. PAYNTER, *Surf. Interface Anal.* **3** (1981) 186.
10. J. E. CASTLE, *Surf. Sci.* **68** (1977) 583.
11. D. K. GILDING, R. W. PAYNTER and J. E. CASTLE, *Biomaterials* **1** (1980) 163.

Received 7 October
and accepted 7 November 1985